The carboxy-terminal region of human lipoprotein lipase is necessary for its exit from the endoplasmic reticulum

Roser Buscà[1,2,*] Mònica Martínez,[2,*] Elisabet Vilella,[†] Julia Peinado,[§] Josep Lluis Gelpi,[§] Samir Deeb,[**] Johan Auwerx,[††] Manuel Reina,[*] and Senén Vilaró[3,*]

Department of Cell Biology,[*] University of Barcelona, Diagonal 645, 08028 Barcelona, Spain; Biomedical Research Center,[†] Hospital St. Joan, 43201 Reus, Tarragona, Spain; Department of Biochemistry and Molecular Biology,[§] University of Barcelona, Diagonal 645, 08028, Barcelona, Spain; Departments of Genetics and Medicine,[**] University of Washington, Seattle, WA 98195; and Laboratorie de Biologie des Régulations chez les Eucaryotes,[††] Department d'Athérosclerose, U325 INSERM, Institut Pasteur, Rue Calmette, 59019 Lille, France

Abstract Certain missense substitutions on the human lipase (hLPL) gene produce mutated proteins that are retained in different compartments along the secretory pathway. The purpose of the present study was to elucidate whether the C-terminal domain of the hLPL molecule could be important for secretion. We constructed by site-directed mutagenesis three carboxy-terminal mutated (F^{388}→Stop, K^{428}→Stop and K^{441}→Stop) hLPL cDNAs that were expressed in COS1 cells. Immunoblotting of cell extracts showed that all three constructs led to similar levels of protein. Both wild type (WT) hLPL and the truncated K^{441}→Stop hLPL were secreted to the extracellular medium, and presented a similar intracellular distribution pattern as shown by immunofluorescence. Neither F^{388}→Stop nor K^{428}→Stop hLPL protein was detected in cell medium. Immunofluorescence experiments showed that both truncated hLPL were retained within an intracellular compartment, which became larger. Double immunofluorescence analysis using antibodies against LPL and antiprotein disulfide isomerase as a marker showed that the truncated K^{428}→Stop hLPL was retained within the rough endoplasmic reticulum. This truncated protein was not found in other compartments in the secretory pathway, such as Golgi complex and lysosomes, indicating that it did not exit the endoplasmic reticulum. Further analysis of the C-terminal region of the LPL molecular model showed both that F^{388}→Stop and K^{428}→Stop hLPL truncated proteins are highly hydrophobic. As retention of secretory proteins in the rough endoplasmic reticulum is a quality control mechanism of the secretory pathway, we conclude that the C-terminal domain of hLPL is critical for correct intracellular processing of the newly synthesized protein.—**Buscà, R., M. Martínez, E. Vilella, J. Peinado, J. L. Gelpi, S. Deeb, J. Auwerx, M. Reina, and S. Vilaró.** The carboxy-terminal region of human lipoprotein lipase is necessary for its exit from the endoplasmic reticulum. J. Lipid Res. 1998. **39:** 821–833.

Supplementary key words lipoprotein lipase • endoplasmic reticulum • carboxy-terminal domain • secretion • intracellular processing • immunofluorescence • structure

Lipid is transported from blood to tissue cells by lipoproteins. Lipoprotein lipase (LPL; E.C. 3.1.1.34) is the rate-limiting enzyme for the hydrolysis and removal of circulating triacylglyceride-rich lipoproteins in blood, such as very low density lipoproteins (VLDL) and chylomicrons (see ref. 1 for a recent review). In addition to its unquestioned role in the hydrolysis of triacylglyceride-rich lipoproteins, it has been recently postulated that LPL could mediate the uptake of chylomicron remnants and VLDL to specific cell-surface receptors in the liver (see refs. 2 and 3 for recent review). Catalytically active LPL is a non-covalent homodimeric glycoprotein, anchored to heparan sulfate proteoglycans on the luminal plasma membrane of capillary endothelia, where it acts on triacylglyceride-rich lipoproteins delivering free fatty acids to parenchymal cells, LPL, like many other secretory proteins, is synthesized at the rough endoplasmic reticulum (rER), from which it is transported to the Golgi complex and further secreted (reviewed in 4). At the rER, human LPL (hLPL) is cotranslationally glycosylated at amino acids Asn^{43} and Asn^{359} (5). Glycosylation of the LPL molecule is required for catalytic activity (6–8) and for release from

Abbreviations: rER, rough endoplasmic reticulum; WT, wild type; ELISA, enzyme-linked immunosorbent assay; PMSF, phenylmethylsulfonylfluoride; HPLC, high performance liquid chromatography; BSA, bovine serum albumin; hLPL, human lipoprotein lipase; VLDL, very low density lipoproteins; FITC, fluorescein isothiocyanate; PDI, protein disulfide isomerase; TRITC, tetramethylrhodamine isothiocyanate; Lampl, lysosome-associated membrane protein; LRP, α_2-macroglobulin receptor/low density lipoprotein receptor-related protein.

[1] Present address: INSERM U385, Faculte de Medecine, 06107, Cedex 02, France.

[2] These authors contributed equally to this paper.

[3] To whom correspondence should be addressed.

the endoplasmic reticulum (9). After initial transfer of a dolichol-P-P to arginine residues, the carbohydrate moiety of the LPL is further assembled to a mannose-rich structure and transported to the Golgi complex, where the oligosaccharides are modified by Golgi-resident enzymes (4). However, Ben-Zeev et al. (7) demonstrated that glucose trimming but not translocation to the *cis*-Golgi compartment is necessary for full catalytic activity of the enzyme, suggesting that the rER is the cellular compartment for proper folding and probably dimerization of the LPL molecule.

LPL, along with pancreatic and hepatic lipase, belongs to the gene family of triglyceride lipases. The three-dimensional structure of LPL has not been determined, but a model of the molecule has been proposed on the basis of its homology with pancreatic lipase (10). On the basis of this model and pioneering biochemical studies (11, 12) LPL can be separated into two folding domains, a larger (three quarters of the sequence) N-terminal (residues 1–312) and a smaller (one quarter) C-terminal domain (residues 313–448) connected by a flexible peptide. Several functional domains are known in the LPL molecule. The N-terminal folding domain comprises: the catalytic triad (Ser^{132}, Asp^{156}, and His^{241}) (13, 14); the lid covering the catalytic triad (residues 216–239) (15), which modulates the interaction with substrates; three positively charged amino acid clusters, which could be binding-sites for heparin and cell surface heparan sulfates (16, 17); and the binding site for the cofactor apoC-II (18). The C-terminal folding domain includes: two sites for binding to α_2-macroglobulin receptor/low density lipoprotein receptor-related protein (hereafter referred to as LRP) (residues 380–384 and 404–430) (19–21); a binding site for heparin and for heparan sulfate proteoglycans (residues 404–430) (21); and a binding site for lipid substrates (tryptophan cluster Trp^{390}–Trp^{393}–Trp^{394}) (22), which confers substrate specificity to the lipase (23–25).

The human LPL gene has a span of 30 kb that comprises 10 exons that code for a 27-amino acid signal peptide and a 448-amino acid mature protein (reviewed in 26–28). Many mutations to the LPL gene have been reported to cause the Type I hyperlipoproteinemia syndrome, which is characterized by an accumulation of chylomicrons in plasma and a marked increase in triacylglyceride levels (29). Most of the genetic defects in the LPL gene are located in exons 5 and 6, which code for amino acids 154 to 285 of the mature protein and correspond to the N-terminal region of the enzyme (27), but some mutations are located within the C-terminal portion. These include two truncated forms of LPL, Trp^{382}→Stop (16, 30) and Ser^{447}→Stop (31) and four missense mutations, Ala^{334}→Thr (32); Glu^{410}→Val (33); Cys^{418}→Tyr (34); Glu^{410}→Lys (35). Some of these mutations lead to abnormal post-heparin LPL activity and mass, suggesting a role of the C-terminal domain in intracellular processing of the molecule.

Recent studies in our laboratory have shown that intracellular processing and secretion of lipoprotein lipase are very sensitive to structural changes. Replacement of Asn^{43} by Ala completely abolishes LPL secretion, leading to the production of inactive LPL, which accumulates inside the rER (9), and replacement of Gly^{142} by Glu leads to a missorted protein, which is diverted to the lysosomes rather than secreted (36). The purpose of this study was to elucidate whether the C-terminal domain of the LPL molecule is important for secretion. To address this question, we constructed, by site-directed mutagenesis, three C-terminal truncated LPLs. We found that cell transfection of F^{38}→Stop and K^{428}→Stop, but not K^{441}→Stop cDNAs produces non-secretable truncated proteins that are retained in the endoplasmic reticulum. This indicates that the C-terminal is critical for correct intracellular processing of the newly synthesized protein in the ER.

MATERIALS AND METHODS

LPL mutagenesis

The three mutant LPL clones were constructed by site-directed mutagenesis. Full-length human LPL was obtained by reverse transcription of RNA, followed by polymerase chain reaction, from THP-1 cells (ATCC T1B202), differentiated with phorbol esters and dexamethasone (37). Human LPL cDNA was cloned in the *Eco* RI site of PTZ18U vector and mutagenized following Kundel, Roberta, and Zakour (38) using the site-directed mutagenesis kit of Bio-Rad. The oligonucleotide primer 5′ G**T GA**T TCA TAC TAG AGC TGG T 3′ used for mutagenesis (Eurogantec, Seraing, Belgium) contained the codon 1477 substitution TTT (Phe) by a TGA (F^{388}→Stop). The oligonucleotide primer 5′ CA TTT GCA G**TG AG**G AAA GG 3′ contained the codon 1537 substitution AAA (Lys) by TGA (K^{428}→Stop), and finally the oligonucleotide primer 5′ GC CAT GAC TAG TCT C**TG A**AT AAG 3′ contained the codon 1576 AAG (Lys) substituted by TGA (K^{441}→Stop). The mutant LPL clones were confirmed by sequencing (Pharmacia). The vector pCAGGS (39, 40), which contains the β-actin promoter and the SV40 replication origin, was used for expression of WT and mutant cDNA hLPL in COS1 cells. The wild type and mutant cDNAs were cloned into the *Eco* RI site.

Cell culture and binding assays

COS1 cells were used for transfection experiments, and human fibroblasts obtained by skin biopsy from a

normal subject were used for binding experiments. Both lines were cultured in Dulbecco's modified Eagle's medium (DMEM), COS1 cells with 4.5 g/l glucose and fibroblasts with 1 g/l. Medium was supplemented with 10% fetal bovine serum (Wittaker, Walkersville, MD), antibiotics and glutamine (2 mm) (Sigma, St. Louis, MO). For heparin treatment, cells were incubated for 6 h with medium containing 100 μg/ml of heparin (Sigma) 48 h post-transfection. For immunofluorescence experiments, cells were cultured in 10-cm plates containing 10 ml of medium. Cells at 80% of confluence were transfected with 2.5 μg of DNA by using the DEAE-dextran chloroquine method (41). LPL binding assays were performed by placing glass coverslips with a subconfluent monolayer of human fibroblasts in a 10-cm dish with COS1 cells transfected with either the WT hLPL or the mutated (F^{388}→Stop, K^{428} →Stop, and K^{441}→Stop hLPL) constructs. Immediately after transfection the coverslips were placed on top of the COS1 cells and both growing cell lines shared the same culture medium, in which the LPL secreted by the transfected cells bind to the surface of the fibroblasts added (42). LPL binding was detected by immunofluorescence as indicated below.

Immunoblotting

COS1 cells were processed 48 h posttransfection. Medium was removed and stored at −70°C. Cells were washed in PBS and collected in a lysis buffer (1% Triton X-100, 1 mm PMSF, 5 mg/ml leupeptin, 2 mm EDTA, 0.5 U/ml aprotinin in PBS). The lysates were scraped from the dishes, passed through a syringe (22 gauge needle), and sonicated for 30 s at maximum power. The lysate was considered as the extract. Cell extracts of transfected cells were loaded into 10% SDS polyacrylamide gel, electrophoresed, and blotted to nitrocellulose (Cellulosenitrat BA8S from Schleicher and Schüll, Dassell, Germany) at 1.5 V for 1.5 h using the semi-dry system of Bio-Rad. The nitrocellulose membranes were blocked with 3% powdered milk in PBS. Medium was loaded into nitrocellulose membranes using the slot-blot system of Bio-Rad. Nitrocellulose was blocked with 5% of powdered milk in PBS. For Western blotting, LPL was detected with polyclonal antibody against recombinant hLPL (36) and secondary peroxidase-conjugated anti-rabbit at 1/2,000 dilution (Dakopatts, Glostrup, Denmark). For slot-blot analysis we used 5D2 monoclonal antibody (43) and secondary peroxidase-conjugated anti-mouse antibody (1:2000) (Dakopatts). Western and slot blot were developed with the ECL system from Amersham (Bucks, UK).

LPL activity and mass in medium

For LPL mass determination in culture medium, we used a solid-phase sandwich ELISA with polyclonal rabbit or chicken antibodies against bovine LPL for coating and 5D2 monoclonal antibody for detection (44). Lipoprotein lipase activity in the medium was determined as described previously (45). One milliunit of lipolytic activity represents the release of 1 nmol fatty acid/min.

Immunofluorescence and confocal microscopy

For immunofluorescence, glass coverslips were washed gently in PBS and fixed with methanol (−20°C) for 2 min. LPL was detected using a monoclonal antibody 5D2 at 1:50 dilution or a polyclonal chicken antibody at 1/200 dilution. As a secondary antibody a fluorescein isothiocyanate (FITC)-conjugated anti-mouse or anti-chicken was used. As markers for intracellular compartments we used: anti-protein disulfide isomerase (PDI) to identify rER, anti-Lamp1 to identify the lysosomal compartment, and anti-β-galactosyltransferase to identify *trans*-Golgi stacks (46). All these antibodies were from rabbit and used at 1:100 dilution. In double immunofluorescence experiments we used a tetramethylrhodamine isothiocyanate (TRITC)-conjugated secondary goat anti-

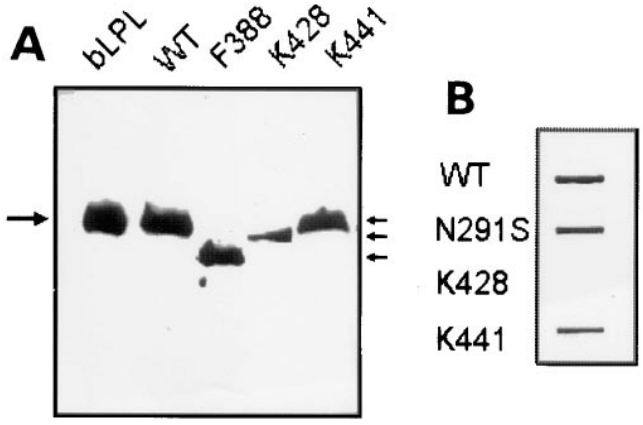

Fig. 1. Immunoblotting of COS1 expressing wild type (WT) or F^{388}→Stop, K^{428}→Stop, and K^{441}→Stop hLPL. A: Western blot of cell extracts from transfected COS1 cells with WT hLPL or the different C-terminal mutated (F^{388}→Stop, K^{428}→Stop and K^{441}→Stop) hLPL cDNAs. Assays were performed 48 h after transfection; 0.2 μg of bovine LPL (bLPL) was used as a control (large arrow, 55 kDa). Equal amounts of protein lysates (30 μg) were loaded into a 10% polyacrylamide gel and transferred to nitrocellulose membrane. Immunodetection was performed with rabbit polyclonal antibody against recombinant hLPL. The apparent molecular masses of the three truncated proteins were lower (small arrows) (around 44 kDa for F^{388}→Stop, 52 kDa for K^{428}→Stop and 56 for K^{441}→Stop) than the WT hLPL (58 kDa). bLPL migrated at 55 kDa. Results are representative of three separate experiments. B: Slot-blot assay of 200 μl of culture media from WT hLPL, N^{291}→S, K^{428}→Stop and K^{441}→Stop hLPL cDNAs transfected cells. The mutated Asn^{291}→Ser ($N^{291}S$) cDNA was used in addition to WT hLPL as a control for LPL normal secretion. Immunodetection was performed with the monoclonal 5D2 antibody. Results are representative of four separate experiments.

mouse at dilution 1:50 (Boehringer Mannheim, Mannheim, Germany) to detect LPL and an FITC-conjugated swine anti-rabbit (Dako Corp. Santa Barbara, CA) at dilution 1:50 to detect the markers for the intracellular compartments. All antibodies were diluted in PBS and 0.5% BSA (Sigma). Fixed cells were incubated with primary antibodies for 45 min at 37°C. Secondary antibodies were applied for 30 min at 37°C. The coverslips were mounted with immunofluorescence medium (ICN Biomedicals Inc., Costa Mesa, CA) and viewed and photographed with 40× or 100× objective using a Reichert Jung Polyvar II microscope equipped with epifluorescence illumination. Confocal microscopy studies were made with a Leica TCS 4D (Leica Lasertechnick GmbH, Heidelberg, Germany) confocal scanning laser microscope adapted to an inverted Leitz DMIRBE microscope. Colocalization analysis was performed by the Multicolor Software (version 2.0, Leica Lasertechnick) (36).

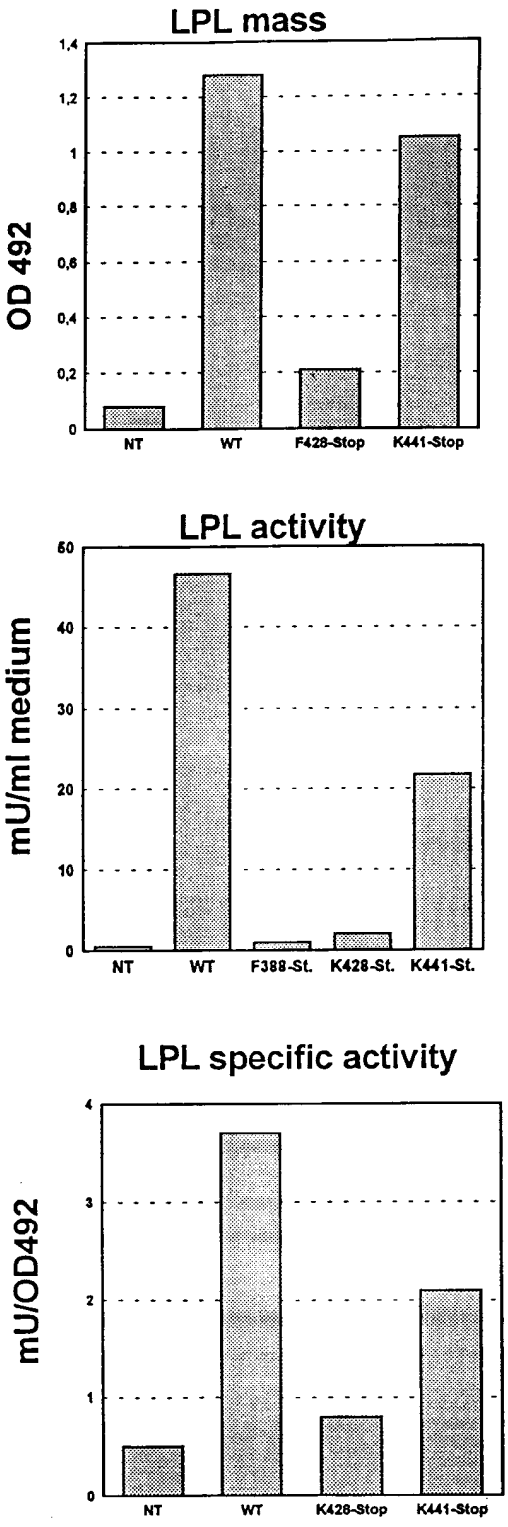

Structural analysis

The C-terminal domain of truncated hLPLs was analyzed using as a template the structural model of LPL proposed by van Tilbeurgh et al. (10). The model was built and manipulated with the molecular modelling package InsightII from Biosym/MSJ at a Silicon Graphics workstation. The energy equivalence of changes in solvent-exposed surfaces was calculated according to the method of Eisenberg and McLachlan (47).

RESULTS

To study the effects of C-terminal truncations on intracellular processing or LPL, COS1 cells were transfected either with WT or with the different C-terminal mutated (F^{388}→Stop, K^{428}→Stop, and K^{441}→Stop) hLPL cDNAs. Assays were performed 48 h after transfection. By Northern blotting of mRNA and hybridization with full-length hLPL labeled probe, we found equal expression of all three constructs (not shown). Western blot analysis of cell extracts (**Fig. 1A**) revealed that all three truncated proteins were expressed by transfected cells. As the epitope recognized by the monoclonal 5D2 antibody is located within residues 396–405 (43), and thus the construction F^{388}→Stop hLPL is not recognized, we used a polyclonal antibody against recombinant hLPL

Fig. 2. LPL mass and activity in culture media of COS1 expressing wild type (WT) or mutated hLPL. COS1 cells were transfected with WT hLPL or with F^{388}→Stop, K^{428}→Stop or K^{441}→Stop hLPL mutant constructions. LPL mass and activity were measured 48 h post-transfection by an ELISA assay using polyclonal antibodies against bLPL for coating and monoclonal 5D2 antibody for detection. Absorbance was measured at 492 nm. The mass of F^{388}→Stop construction was not measured in medium because the truncated protein does not include 5D2 recognized epitope. Medium was collected and LPL activity was measured as described under Materials and Methods according to standard procedures. The results are representative of three separate experiments.

(36). As expected, the apparent molecular mass of the three proteins was lower (around 44 kDa for F^{388}→Stop, 52 kDa for K^{428}→Stop, and 56 kDa for K^{441}→Stop) than the WT hLPL (58 kDa), which was similar to bovine LPL (55 kDa). This result indicates that similar levels of expression of the truncated proteins were shown by transfected cells and also that the size of the proteins was as expected. To determine whether the truncated proteins are secreted by the transfected cells, we performed slot-blot assays (Fig. 1B) in culture media collected 48 h after transfection using the monoclonal antibody 5D2, which is more sensitive than the rabbit polyclonal antibody. Unfortunately, as stated above, the construct F^{388}→Stop hLPL was not recognized by the 5D2 antibody (not shown). As a control for normal LPL secretion we used cells transfected with either WT or Asn^{291}→Ser ($N^{291}S$) constructs, which are normally secreted by COS cells (42). K^{428}→Stop was not detected in the cell medium, while the K^{441}→Stop was secreted. Parallel immunoblotting experiments of the cell media and binding assays on human fibroblasts (not shown) using the polyclonal antibodies confirmed this result and suggested that neither F^{388}→Stop hLPL nor K^{428}→Stop hLPL was secreted by expressing cells. To confirm the impaired secretion of the K^{428}→Stop hLPL truncated protein, mass and enzymatic activity in media from transfected cells were measured (**Fig. 2**). ELISA assay with the 5D2 antibody showed that the truncated K^{428}→Stop hLPL mass was very low in cell culture media. The truncated K^{441}→Stop hLPL presented around 80% of the activity detected by the WT hLPL. The calculated specific activity of this truncated form was approximately 55% of the secreted WT hLPL. The detectable activity of the F^{388}→Stop and K^{428}→Stop hLPLs was negligible.

It is well known that heparin increases the rate of LPL secretion in several cell types (4). Here we examined whether cell release of the C-terminal truncated hLPL was sensitive to heparin. In WT hLPL transfected cells, heparin doubled the level of extracellular mass of LPL as detected by ELISA using the polyclonal-5D2 method (44) (**Fig. 3A**). In contrast, in cells transfected with both K^{428}→Stop and K^{441}→Stop hLPL cDNAs, heparin did not increase the amount of extracellular LPL. This indicated that the retained K^{428}→Stop hLPL could not be released by heparin treatment.

To identify the cell compartment in which the truncated forms of hLPL were retained, we performed immunofluorescence using the 5D2 monoclonal antibody to detect WT, K^{428}→Stop, and K^{441}→Stop hLPLs, and chicken polyclonal antibody against bovine LPL to detect the F^{338}→Stop hLPL construct. Previous reports from our laboratory demonstrated that both antibodies can be used to detect expressed hLPL inside transfected cells by immunofluorescence (9). **Figure 4** shows the results of such analysis. The immunofluorescence pattern was similar for cells transfected with WT hLPL (Fig. 4A) or K^{441}→Stop hLPL (Fig. 4D), showing a fine reticular staining throughout the cytoplasm and surrounding the nucleus, which mostly corresponds to the rough endoplasmic cisternae (9). Part of the perinuclear staining corresponded to Golgi cisternae (see below). In contrast, COS1 cells expressing either F^{388}→Stop (Fig. 4B) or K^{428}→Stop (Fig. 4C) appeared wrinkled and presented large regions of intense immunofluorescence staining, suggesting that both F^{388}→Stop and K^{428}→Stop were retained within an intracellular compartment, and that the large accumulation of expressed protein changed the shape of the cell.

Next we performed double labeling experiments using markers for rER (anti-PDI) (**Fig. 5**), Golgi stacks (anti-β-galactosyltransferase) and lysosomes (anti-Lamp1) (**Fig. 6**). The only antibodies available against these compartment-specific proteins are from rabbit, thus for

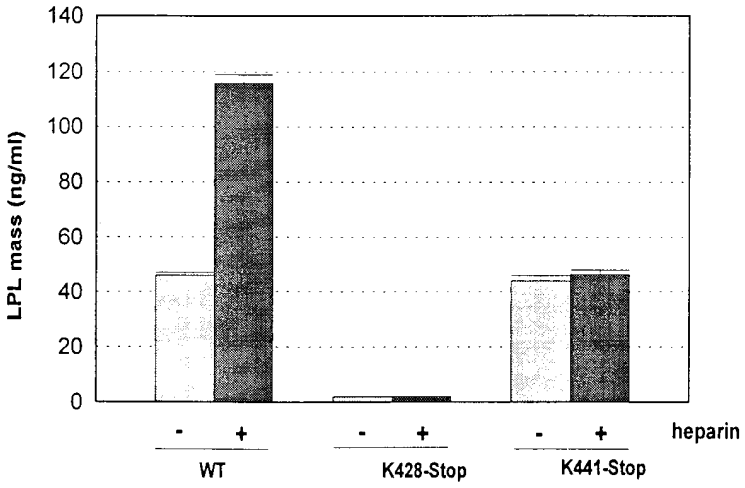

Fig. 3. Effects of heparin on the secretion of K^{428}→Stop or K^{441}→Stop hLPL from COS1 transfected cells. LPL mass in medium of COS1 transfected cells treated with heparin. Forty-eight h after transfection, medium was removed from plates and fresh medium supplemented with or without 10 U/ml of heparin was added. Cells were incubated for a further 6 h. LPL mass in medium was measured by a solid phase ELISA polyclonal anti-bLPL for coating monoclonal 5D2 antibody for detection as in Fig. 2. Purified bLPL was used as a concentration reference line. Values are indicated as mean ± SEM (n = 4).

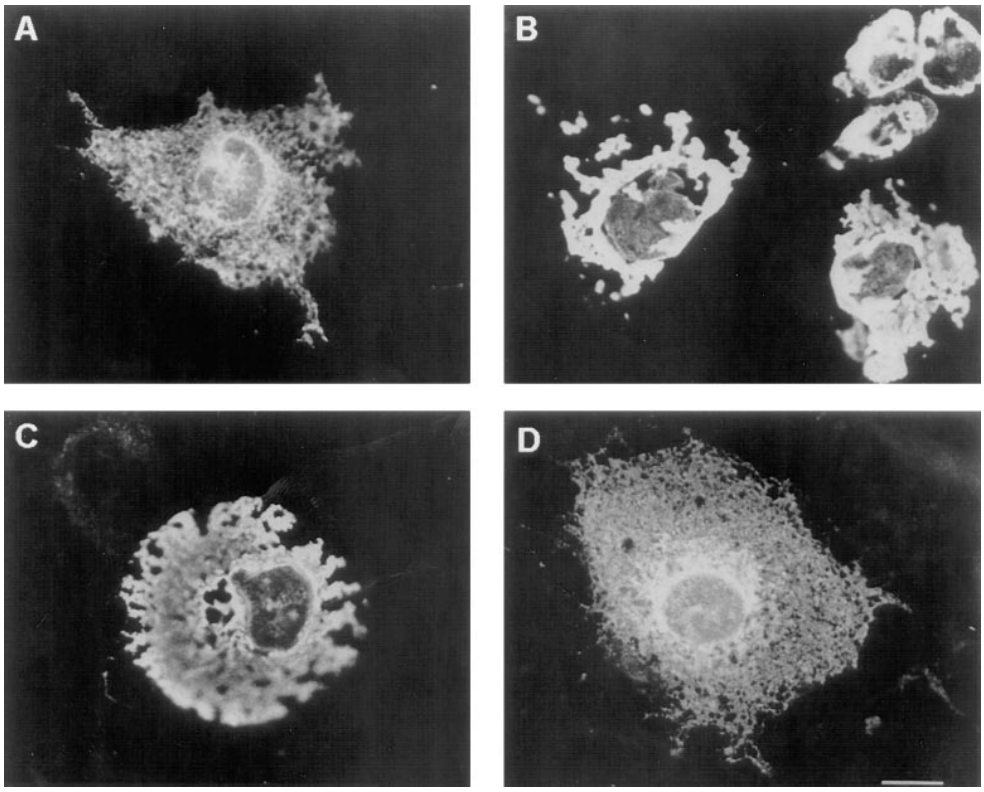

Fig. 4. Immunofluorescence distribution of WT, F^{388}→Stop, K^{428} Stop and K^{441}→Stop hLPL in COS1 transfected cells. Transfected cells were fixed 48 h after transfection. Immunofluorescence was performed using 5D2 monoclonal antibody to detect WT (A), K^{428}→Stop (C) and K^{441}→Stop (D) hLPLs, and chicken polyclonal antibody against bovine LPL to detect the F^{388}→Stop hLPL construct. Monoclonal antibodies were stained with FITC-conjugated goat anti-mouse. (B) Note that the immunofluorescence pattern was similar for the F^{388}→Stop and K^{428}→Stop hLPL-expressing cells and for the WT and K^{441}→Stop hLPL-expressing cells. Bar: 30 μm.

the double immunofluorescence experiments we could only use the monoclonal 5D2 but not the polyclonal antibodies against LPL to detect the hLPL. Consequently, by this approach, we could not study the truncated F^{388}→Stop hLPL. As previously described (9, 36), double immunofluorescence with 5D2 and anti-PDI indicated that in WT hLPL-transfected cells, most of the immunostained protein is present within the endoplasmic reticulum (Fig. 5A and B). In these LPL-secreting cells, anti-PDI stained a fine reticular structure that extends from the perinuclear area towards the periphery of the cells (Fig. 5B). A large proportion of the LPL colocalizes with anti-PDI in this reticular structure. However, in K^{428}→Stop hLPL-transfected cells, the rER (as stained by the anti-PDI) no longer presented a reticular appearance (Fig. 5D); rather it was enlarged, occupying a large proportion of the cytoplasm of the transfected cells. The immunofluorescence distribution of the truncated K^{428}→Stop totally coincided with the anti-PDI immunostaining (Fig. 5C and D), indicating that the truncated protein was retained in the rER and suggesting that the LPL accumulation induces an enlargement of this compartment. Parallel immunolocalization experiments performed with markers of the Golgi apparatus and lysosomes (Fig. 6) further demonstrated that K^{428}→Stop hLPL was not found in these compartments, reinforcing the conclusion that the truncated C-terminal protein was retained in the endoplasmic reticulum.

The structural implications of the truncation of LPL at the residues F^{388}→Stop and K^{428}→Stop were analyzed by molecular modelling on the basis of the homology model reported by van Tilbeurgh et al. (10). The C-terminus domain of hLPL is constituted by an 8-strand β-barrel with a compact core of hydrophobic residues. F^{388} is located at a surface loop between the strands β5 and β6, and K^{428} is at the beginning of a β8 strand (**Fig. 7A**). Provided that hLPL could maintain a native-like fold, the truncation of the protein would lead to a 5-strand barrel for F^{388}→Stop hLPL and a 7-

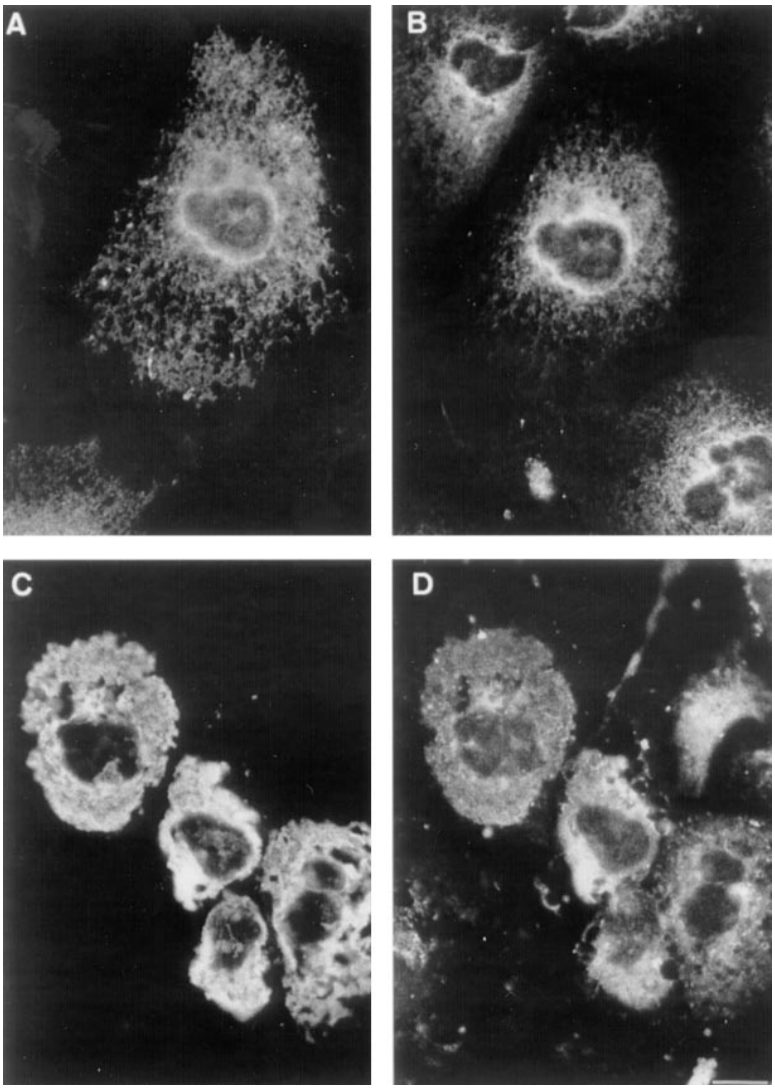

Fig. 5. Truncated K^{428}→Stop hLPL accumulates within the rough endoplasmic reticulum. COS1 cells were transfected with WT hLPL (A and B) or K^{428}→Stop hLPL (C and D) and double immunofluorescence, using the monoclonal 5D2 antibody to detect LPL protein (A and C) and a rabbit polyclonal antibody to detect protein disulfide isomerase as a marker of rough endoplasmic reticulum (B and D), was performed as indicated in Materials and Methods. Monoclonal antibodies were stained with TRITC-conjugated goat anti-mouse immunoglobulins and polyclonal antibodies with FITC-conjugated swine anti-rabbit immunoglobulins. Note that the immunofluorescence staining of the K^{428}→ Stop hLPL totally coincides with the PDI distribution of transfected cells. The endoplasmic reticulum of K^{428}→Stop hLPL transfected cells appeared enlarged. Bar: 30 μm.

strand barrel for K^{428}→Stop hLPL. Both structures are expected to be unstable. At this point, two main effects may contribute to the destabilization of the C-terminal domain. On one hand, the disruption of the β-sheet structure, and, on the other, the exposure of a number of hydrophobic residues. Figure 7a shows the contribution of the eliminated residues to the hydrogen-bond pattern of the β-barrel. K^{428}→Stop hLPL would have the connection between β5 and β7 disrupted (4 hydrogen bonds). The changes in F^{388}→Stop hLPL are more significant as three complete strands are removed, leaving strands β1 and β5 disconnected (11 hydrogen bonds). In both cases there is a significant exposure of the hydrophobic core of the β-barrel to the solvent. To evaluate the energetic implication of these changes, three models of the C-terminal domain (WT, F^{388}→ Stop, and K^{428}→Stop hLPL) were built from the model proposed by van Tilbeurgh (10). No optimization was

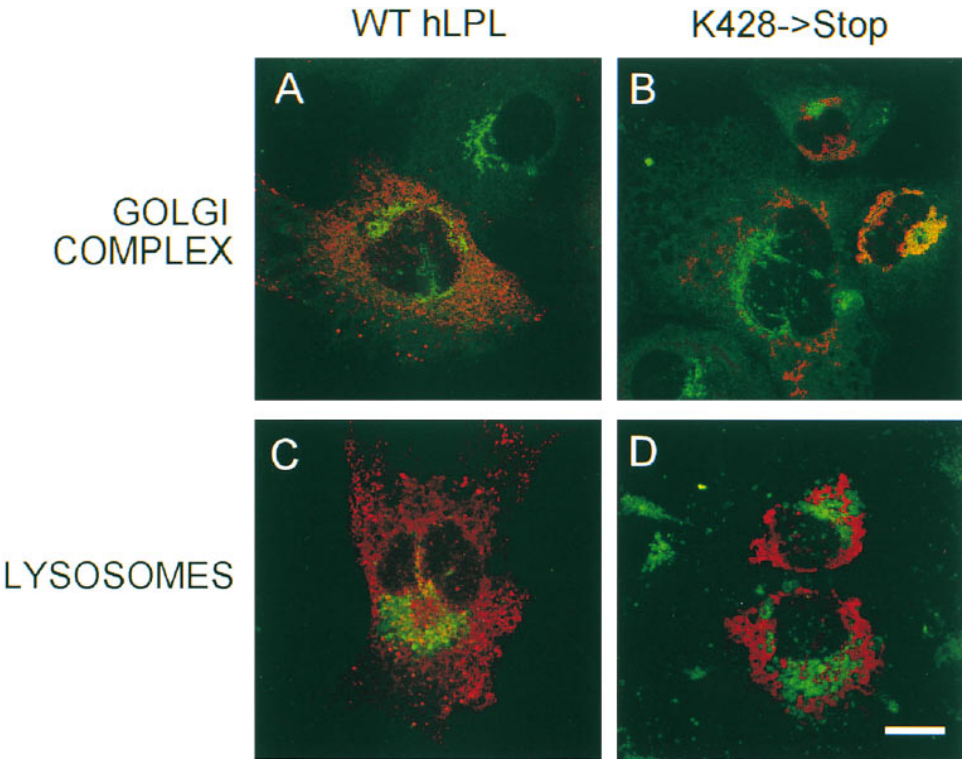

Fig. 6. Truncated K^{428}→Stop does not reach the Golgi complex nor lysosomes. COS1 cells were transfected with WT hLPL (A and C) or K^{428}→Stop hLPL (B and D) and double immunofluorescence, using the monoclonal 5D2 antibody to detect LPL protein (A, B, C, and D) and rabbit polyclonal antibodies against β-galactosyltransferase as a marker Golgi complex (A and B) or rabbit polyclonal antibodies against Lamp1 as a marker for lysosomes (C and D). Monoclonal antibodies were stained with TRITC-conjugated goat anti-mouse immunoglobulins (red) polyclonal antibodies with FITC-conjugated swine anti-rabbit immunoglobulins (green). Images were obtained using confocal microscopy as indicated under Materials and Methods. A single optical section taken in the middle of the cells is shown (0.3 μm; pixel size (*x*, *y*) 0.2 μm. The panels show a superimposed image of the fluorescence signal obtained from green and red channels. Panel B shows three transfected cells presenting different levels of K^{428}→Stop hLPL expression. The cell with a highest expression (orange color) appeared wrinkled. Bar: 30 μm.

performed as they were not intended to represent actual proteins but only to estimate the contribution to stability of the sequences removed. Figure 7B shows changes in solvent exposed surface from the native protein to the truncated hLPLs. Evaluation of the energetic equivalence of these changes according to the method of Eisenberg and McLachlan (47) indicated that the hydrophobic core of a "correctly folded" F^{388}→Stop hLPL would be 13.1 kcal/mol less stable than the native protein. This change was due mainly to the exposure of Leu^{375}, Leu^{378} and Leu^{380}, Trp^{382}, Phe^{335} and Phe^{322}, Tyr^{316} Ile^{320} and Ile^{337} otherwise covered by strands β6 and β7. Changes in K^{428}→Stop hLPL were less significant, as expected. The hydrophobic core of K^{428}→Stop hLPL would be "only" 4.4 kcal/mol less stable than the native protein, due to Phe^{417}, Cys^{418}, Leu^{380}, and Ile^{404}. An important feature of K^{428}→Stop hLPL is that Cys^{418} is completely solvent exposed (Fig. 7A). This residue together with Cys^{438} (missing in K^{428}→Stop hLPL) forms a disulfide bridge in WT hLPL.

DISCUSSION

An increasing body of experimental evidence indicates that the C-terminal folding domain of the LPL molecule, which comprises residues 313–448, plays an important role in the structure–function properties of this enzyme. It contains two binding sites for LRP (19–21); a binding site for heparin and heparan sulfate proteoglycans (21); and a binding site for lipoproteins (12, 22, 48). Several quality control mechanisms ensure that

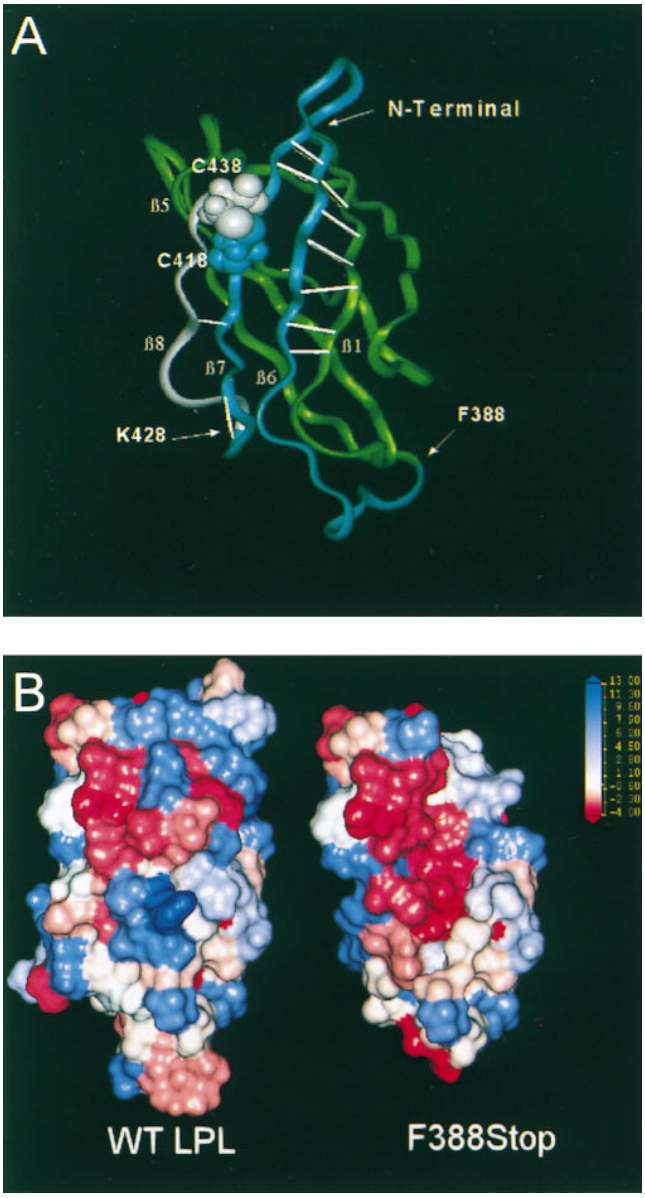

Fig. 7. Structure of the C-terminal domain of hLPL. A: Ribbon presentation including main chain hydrogen bounds (white lines) involving strands β6 to β8. Green: F^{314}–Y^{387}, F^{388}–Q^{427}, and white K^{428}–C^{448}, C^{418} and C^{438}, involved in the disulfide bond, are represented as solid fill models. B: Solvent-exposed surfaces of WT and F^{388}→Stop hLPL C-terminal domain. Surfaces are colored according to the hydrophobicity of the residues involved. More negative values (red) correspond to the most hydrophobic residues. Scale in B indicates the relative hydrophobicity.

only properly folded proteins are secreted or exposed to the cell surface. The rER controls the quality of folding intermediates, incompletely assembled proteins, misfolded proteins, and aggregated side products, which are selectively retained within this compartment (49). Previous studies have demonstrated that some missense substitutions on the LPL gene produce mutated proteins that are retained in different compartments along the secretory pathway (9, 36). Here we present evidence that the C-terminal domain of the LPL is also critical to the release of the molecule from the rER, which suggests that in the absence of a domain portion, the molecule could not be correctly folded and would be retained in the cell.

The results obtained in the present study indicate that deletion of the last 61 (F^{388}→Stop hLPL) and 21 (K^{428}→Stop hLPL) amino acids produces truncated LPL proteins that cannot be efficiently secreted by expressing cells and that therefore accumulate inside the rER (as shown by double immunofluorescence experiments). Although F^{388}→Stop hLPL was not studied in the same detail, because of the loss of the monoclonal 5D2 recognized epitope at the C-terminal domain, our data indicate that this mutant is also retained at the rER to the same extent as K^{428}→Stop hLPL. This is supported by the immunofluorescence studies with polyclonal antibodies, which showed an identical retention pattern of intracellular LPL in F^{388}→Stop and K^{428}→Stop hLPL-expressing cells. Previous studies by Kozaki et al. (50) have demonstrated that truncated LPLs not longer than 435 amino acids, when expressed in cultured cells, appear to have some functional impairment, as both mass and activity were reduced as the mutant LPL became smaller. In their study (50), the authors suggested that this could be due to a reduced rate of protein expression. Here, both Northern and Western blotting showed that the lack of detectable mass in culture medium from cells transfected with the shorter LPL mutants could not be a consequence of a low level of expression. In addition, immunofluorescence showed a huge amount of immunoreactive material inside transfected COS1 cells (Fig. 4). Thus, it is very likely that a defect in intracellular processing of the two truncated LPL induces their retention within the cells. In contrast to the shorter LPL mutants, we found that the truncated K^{441}→Stop hLPL was efficiently secreted by transfected COS1 cells.

Analysis of the molecular model of the LPL, generated by van Tilbeurgh et al. (10), we suggested several reasons for the intracellular retention of both truncated forms of LPL. The C-terminal domain of the LPL molecule has a β-sandwich fold with a highly compact hydrophobic core. Truncation of LPL at residue F^{388} has two main consequences. The overall layout of the β-sheet is severely distorted as three of the eight β-strands are removed. This leads to the loss of the hydrogen bond connection and gives an open 5-strand barrel. It can be argued that an alternative fold would give an equally stable 5-strand β structure by connecting strands β1 and β5 (see Fig. 7). However, visual inspection of the hydrophobic core of the original fold clearly

shows that this is not possible without a significant number of van der Waals collisions between the bulky hydrophobic side chains. On the other hand, 5-strand β-barrels are rare in nature (51). To evaluate the stability of this hypothetical open structure, we have analyzed solvation energies. Using the method of Eisenberg and McLachlan (47), the decrease in stability of the hydrophobic core of the C-terminal domain of F^{388}→Stop was calculated as 13.1 kcal/mol. This could be understood as a difference in the contribution of the hydrophobic effect to the protein stability. As this value is of the same order of magnitude as the folding energy of an entire protein, the main conclusion is that the C-terminal domain of the F^{388}→Stop hLPL protein would not have sufficient driving force to fold into a native-like structure, as a significant amount of the hydrophobic surface would still be in contact with solvent. A deficient folding of this domain has different consequences, depending on the environment. The C-terminus domain of LPL may not be necessary for the catalytic activity in vitro. Indeed, purified bovine LPL can be cleaved by mild chymotrypsin treatment between Phe^{390} and Ser^{391} and between Trp^{392} and Ser^{393} (bovine LPL is two residues longer than its human counterpart) and the truncated protein retains several catalytic properties (12). However, in vivo, a misfolded C-terminal domain can compromise the processing of the entire protein in the rER.

The same kind of analysis was performed on the K^{428}→Stop hLPL model. In this case, the distortion of the β-barrel is less important, as only one strand is missing. This means that only the hydrogen-bond connectivity involving β8 is disrupted. The analysis of changes in hydrophobic solvation energy also reveals a much lower destabilization energy (4.4 kcal/mol). This suggests that a very unstable 7-strand β-barrel with a native-like structure would still be possible. However, there is another structural feature to be considered. As stated above, K^{428} is located in the middle of the Cys^{418}/Cys^{428} disulfide bridge. The truncated K^{428}→Stop hLPL has an unpaired Cys^{418}, leading to the presence of a fully exposed sulfhydryl group. LPL contains four disulfide bridges, three of which are located at the N-terminal domain, and the fourth at the C-terminal domain. A recent report (34) described a compound heterozygous patient carrying Ile^{194}→Thr and Cys^{418}→Tyr substitutions. This latter missense mutation destroys the disulfide bridging in the C-terminal domain. The patient showed almost complete catalytic deficiency and very low post-heparin LPL mass. COS1 cells transfected with the Cys^{418}→Tyr variant generated by site-directed mutagenesis produce LPL whose mass and activity were about half of that produced by WT hLPL transfected cells. However, the cysteine mutant pair (Cys^{41}→Ser/Cys^{43}→Ser, which eliminates the disulfide bridge, also shows lower secretable LPL mass but higher specific activity (34, 52). Sequence comparison shows that this C-terminal disulfide bond is completely conserved across evolution, suggesting an important role of LPL domain function. Whether the loss of the disulfide bridge leads to further destabilization by itself or whether the newly available Cys^{418} is modified by oxidation and recognized by a specialized cell machinery remains to be determined. However, once more, a truncated hLPL that hypothetically fails to fold in the proper structure appears to be selectively retained by the cell.

Our understanding of how the cell recognizes and distinguishes between properly folded and incomplete proteins is only partial. However, there is accumulating evidence that several quality control mechanisms operate within the secretory pathway. One level of control, which may operate for rER retention of F^{388}→Stop hLPL, is mediated by resident endoplasmic chaperones, which bind and retain incompletely or improperly assembled proteins, thus preventing their transport through secretory pathway (53, 54). Another mechanism, which could operate for the intracellular retention of K^{428}→Stop hLPL found in the present study, blocks the protein release from the endoplasmic reticulum by thiol-mediated retention, which is believed to monitor the oxidation status of one or more cysteines (55) until polymerization has been completed. This is the case of the polymeric IgM, whose assembly intermediates are retained within the ER by means of a C-terminal cysteine (56, 57). A third mechanism recognizes and retains large protein hydrophobic aggregates (58). The hydrophobic surface exposed by the truncated C-terminal domain could induce aggregation of LPL at the endoplasmic reticulum, which would impair its further intracellular transport and processing. Nevertheless, while the misfolding and/or aggregation of the truncated LPL is likely to be the cause of the ER retention, further studies are necessary to elucidate the mechanism(s) responsible for such ER accumulation.

The mutant K^{441}→Stop hLPL was efficiently secreted by COS1-expressing cells. Previous results obtained by others (48, 52), demonstrated that truncated LPL longer than 437 residues are normally secreted by transfected COS1 cells. Taken together, these suggest that the lack of the last nine or ten amino acids does not produce marked conformational effects. From the structural point of view, K^{441}→Stop hLPL cannot be studied using van Tilbeurgh's model (10), as the last 10 residues are missing. However, it seems evident that the structural integrity of the C-terminal β-sandwich is not compromised, as the 8th β-strand finishes with residue Cys^{438}. Changes beyond this point are expected to have little effect on the overall folding. However, the low spe-

cific activity shown by this truncated LPL suggests that the last amino acids could have some influence on the overall function of the LPL molecule. The truncation may affect the tryptophan cluster (Trp^{390}–Trp^{393}–Trp^{394}) (22) that contributes to the binding of LPL to lipid/water interfaces. However, it cannot be ruled out that the last amino acid residues could influence the stability of the homodimeric structure of LPL (25).

Some Type I hypertriacylglyceridemic patients carrying mutations in the C-terminal domain of the LPL present defects in both post-heparin enzymatic activity and mass. Among them a patient carrying a nonsense mutation in exon 8 (Trp^{382}→Stop) presented very low levels of LPL mass in post-heparin plasma (30, 59). Furthermore, a C-terminal truncation of LPL at residue 381 caused a loss of catalytic activity as well as a decrease in protein mass in transient transfection studies (50). Our results obtained with the K^{388}→Stop hLPL truncated form allowed us to hypothesize that the lack of detectable mass could be a consequence of rER retention and perhaps degradation of the protein. Homozygous missense mutations in Ala^{334}→Thr (32) produce a 50% reduction of the post-heparin mass of normal subjects and nearly absent lipolytic activity. This again emphasizes the importance of the C-terminal region of the LPL in relation to secretion and its role in enzymatic activity. Consistent with this hypothesis, a C-terminal disruption of LPL in mice is lethal in homozygotes and causes hyperlipidemia in heterozygotes (60). It is thus likely that disturbance of the C-terminal domain, in addition to altering the catalytic activity, also alters the intracellular processing of the LPL, causing Type I hyperlipoproteinemia. Together with the present findings these data led us to postulate that, in addition to binding to cell-surface receptors and lipid substrates, the C-terminal domain of the LPL is important for the co- or post-translational processing of the molecule that occurs in the rough endoplasmic reticulum.

We thank Dr. Herman van Tilbeurgh for the coordinates of the LPL structural model. We also thank Dr. Gunilla Olivecrona for providing the bovine LPL and affinity-purified chicken anti-LPL immunoglobulins, Dr. Sven Carlsson for the anti-Lamp1 antibodies, Dr. Gustavo Egea for the anti-PDI and anti-β-galactosyltransferase, Josep Julve for helping in activity assays, Miguel Angel Pujana for his work in the cloning of the WT and mutant LPL in the expressing vector pCAGGS. We are indebted to Susanna Castel for her expert assistance in the confocal microscopy. We are especially grateful to David Garcia for his technical help in the cell care and to Robin Rycroft for his expert editorial help. This work was supported by the Comisión Interministerial de Ciencia y Tecnologia (grant PB94-1548), the Fondo de Investigaciones Sanitarias from Ministerio de Sanidad (grant 96/2099), Association pour la Recherche contre le Cancer (ARC) and the European Community (BIOMED PL-921243).

Manuscript received 5 August 1997 and in revised form 18 December 1997.

REFERENCES

1. Goldberg, I. J. 1996. Lipoprotein lipase and lipolysis: central roles in lipoprotein metabolism and atherogenesis. *J. Lipid. Res.* **37:** 693–707.
2. Olivecrona, G., and T. Olivecrona. 1995. Triglyceride lipases and atherosclerosis. *Curr. Opin. Lipidol.* **6:** 291–305.
3. Beisiegel, U. 1995. Receptors for triglyceride-rich lipoproteins and their role in lipoprotein metabolism. *Curr. Opin. Lipidol.* **6:** 117–122.
4. Braun, J. E. A., and D. L. Severson. 1992. Regulation of the synthesis, processing and translocation of lipoprotein lipase. *Biochem. J.* **287:** 337–347.
5. Hide, W. A., L. Chan, and W. H. Li. 1992. Structure and evolution of the lipase superfamily. *J. Lipid. Res.* **33:** 167–178.
6. Semenkovich, D. F., C. C. Luo, M. K. Nakanishi, S-H. Chen, L. C. Smith, and L. Chan. 1990. In vitro expression and site-specific mutagenesis of the cloned human lipoprotein lipase gene. *J. Biol. Chem.* **265:** 5429–5433.
7. Ben-Zeev, O., M. H. Doolittle, R. C. Davis, J. Elovson, and M. C. Schotz. 1992. Maturation of lipoprotein lipase. *J. Biol. Chem.* **267:** 6219–6227.
8. Ben-Zeev, O., G. Stahnke, G. Liu, R. C. Davis, and M. H. Doolittle. 1994. Lipoprotein lipase and hepatic lipase: the role of asparagine-linked glycosylation in the expression of a functional enzyme. *J. Lipid. Res.* **35:** 1511–1523.
9. Buscà, R., M. Pujama, P. Pognonec, J. Auwerx, S. S. Deeb, M. Reina, and S. Vilaró. 1995. Absence of N-glycosylation at asparagine 43 in human lipoprotein lipase induces its accumulation in the rough endoplasmic reticulum and alters this cellular compartment. *J. Lipid. Res.* **36:** 939–951.
10. Van Tilbeurgh, H., A. Roussel, J-M. Lalouel, and C. Cambillau. 1994. Lipoprotein lipase. Molecular model based on the pancreatic lipase X-ray structure: consequences for heparin binding and catalysis. *J. Biol. Chem.* **269:** 4626–4633.
11. Bengtsson-Olivecrona, G., T. Olivecrona, and H. Jörnvall. 1986. Lipoprotein lipases from cow, guinea-pig and man. *Eur. J. Biochem.* **161:** 291–288.
12. Lookene, A., and G. Bengtsson-Olivecrona. 1993. Chymotryptic cleavage of lipoprotein lipase. *Eur. J. Biochem.* **213:** 185–194.
13. Emmerich, J., O. U. Beg, J. Peterson, L. Previato, J. D. Brunzell, H. B. Brewer, and S. Santamarina-Fojo. 1992. Human lipoprotein lipase. Analysis of the catalytic triad by site-directed mutagenesis of Ser-132, Asp-156 and His-241. *J. Biol. Chem.* **267:** 4161–4165.
14. Faustinella, F., A. Chang, and J. P. Van Biervlet. 1991. Catalytic triad residue mutation (Asp156→Gly), causing familial lipoprotein lipase deficiency: co-inheritance with a nonsense mutation (Ser447→Ter in a Turkish family). *J. Biol. Chem.* **266:** 14418–14424.
15. Dugi, K. A., H. L. Dichek, and S. Santamarina-Fojo. 1995. Human hepatic and lipoprotein lipase. The loop covering the catalytic site mediates lipase substrate specificity. *J. Biol. Chem.* **270:** 25396–25401.
16. Ma, Y., H. E. Henderson, M-S. Liu, H. Zhang, I. J. Forsythe, L. Clarke-Lewis, M. R. Hayden, and J. D. Brunzell.

1994a. Mutagenesis in four candidate heparin binding regions (residues 279–282, 291–304, 390–393, and 439–448) and identification of residues affecting heparin binding of human lipoprotein lipase. *J. Lipid. Res.* **35:** 2049–2059.
17. Hata, A., D. N. Ridinger, S. Sutherland, M. Emi, Z. Shuhua, R. L. Myers, K. Ren, T. Chen, I. Inoue, D. E. Wilson, P-H. Iverius, and J-M. Lalouel. 1993. Binding of lipoprotein lipase to heparin. Identification of five critical residues in two distinct segments of the amino-terminal domain. *J. Biol. Chem.* **268:** 8447–8457.
18. Yang, C-Y., Z-W. Wu, H-X. Yang, M. F. Rohde, A. M. Gotto, and H. J. Pownall. 1989. Structure of bovine milk lipoprotein lipase. *J. Biol. Chem.* **264:** 16822–16827.
19. Williams, S. E., I. Inoue, H. Tran, G. L. Fry, M. W. Pladet, P-H. Iverius, J-M. Lalouel, D. A. Chappell, and D. K. Strickland. 1994. The carboxyl-terminal domain of lipoprotein lipase binds to the low density lipoprotein receptor-related protein / α_2-macroglobulin receptor (LRP) and mediates binding of normal very low density lipoprotein to LRP. *J. Biol. Chem.* **269:** 8653–8658.
20. Nykjaer, A., M. Nielsen, A. Lookene, N. Meyer, H. Roigaard, M. Etzerodt, U. Beisiegel, G. Olivecrona, and J. Gliemann. 1994. A carboxyl-terminal fragment of lipoprotein lipase binds to the low density lipoprotein receptor-related protein and inhibits lipase-mediated uptake of lipoprotein in cells. *J. Biol. Chem.* **269:** 31747–31755.
21. Nielsen, M. S., J. Brejning, R. García, H. Zhang, M. R. Hayden, S. Vilaró, and J. Gliemann. 1997. Segments in the C-terminal folding domain of lipoprotein lipase important for binding to the low density lipoprotein receptor-related protein and to heparan sulfate proteoglycans. *J. Biol. Chem.* **272:** 5821–5827.
22. Lookene, A., N. B. Groot, J. J. P. Kastelein, G. Olivecrona, and T. Bruin. 1997. Mutation of tryptophan residues in lipoprotein lipase. Effects on stability, immunoreactivity, and catalytic properties. *J. Biol. Chem.* **272:** 766–772.
23. Wong, H., R. C. Davis, J. Nikazy, K. E. Seebart, and M. C. Schotz. 1991. Domain exchanger: characterization of a chimeric lipase of hepatic lipase and lipoprotein lipase. *Proc. Natl. Acad. Sci. USA.* **88:** 11290–11294.
24. Davis, R. C., H. Wong, J. Nikazy, K. Wang, Q. Han, and M. C. Schotz. 1992. Chimeras of hepatic lipase and lipoprotein lipase: domain localization of enzyme-specific properties. *J. Biol. Chem.* **267:** 21499–21504.
25. Wong, H., R. C. Davis, T. Thuren, J. W. Goers, J. Nikazy, M. Waite, and M. C. Schotz. 1994. Lipoprotein lipase domain function. *J. Biol. Chem.* **269:** 10319–10323.
26. Auwerx, J., P. Leroy, and K. Schoonjans. 1992. Lipoprotein lipase: recent contributions from molecular biology. *Crit. Rev. Clin. Lab. Sci.* **29:** 243–268.
27. Santamarina-Fojo, S. 1992. Genetic dyslipoproteinemias: role of lipoprotein lipase and apolipoprotein C-II. *Curr. Opin. Lipidol.* **3:** 186–195.
28. Santamarina-Fojo, S., and K. A. Dugi. 1994. Structure, function and role of lipoprotein lipase in lipoprotein metabolism. *Curr. Opin. Lipidol.* **5:** 117–125.
29. Brunzell, J. D. 1989. Familial lipoprotein lipase deficiency and other causes of the chylomicronemia syndrome. *In* The Metabolic Basis of Inherited Disease. 6th ed. C.R. Scriver, A.L. Beaudet, W.S. Sly and D. Valle, editors. McGraw Hill, New York, 1165–1180.
30. Gotoda, T., N. Yamada, M. Kawamura, K. Kozaki, N. Mori, S. Ishibashi, H. Shimano, F. Takaku, Y. Yazaki, Y. Furuichi, and T. Murase. 1991. Heterogeneous mutations in the human lipoprotein lipase gene in patients with familial lipoprotein lipase deficiency. *J. Clin. Invest.* **88:** 1856–1864.
31. Kobayashi, J., T. Nishida, D. Ameis, G. Stahnke, M. C. Schotz, H. Hashimoto, I. Fukamachi, K. Shirai, Y. Saito, and S. Yoshida. 1992. A heterozygous mutation (the codon for $Ser^{447}\rightarrow$ a stop codon) in lipoprotein lipase contributes to a defect in lipid interface recognition in a case with type I hyperlipidemia. *Biochem. Biophys. Res. Commun.* **182:** 70–77.
32. Kobayashi, N. Sasaki, J. Tashiro, H. Inadera, Y. Saito, and S. Yoshida. 1993. A missense mutation ($Ala^{334}\rightarrow$Thr) in exon 7 of the lipoprotein lipase gene in a case with type I hyperlipidemia. *Biochem. Biophys. Res. Commun.* **191:** 1046–1054.
33. Previato, L., O. Guardamagna, K. A. Dugi, R. Ronan, G. D. Talley, S. Santamarina-Fojo, and H. B. Brewer. 1994. A novel missense mutation in the C-terminal domain of lipoprotein lipase ($Glu^{410}\rightarrow$Val) leads to enzyme inactivation and familial chylomicronemia. *J. Lipid. Res.* **35:** 1552–1560.
34. Henderson, H. E., F. Hassan, D. Marais, and M. R. Hayden. 1996. A new mutation destroying disulphide bridging in the C-terminal domain of lipoprotein lipase. *Biochem. Biophys. Res. Commun.* **227:** 189–194.
35. Wiebusch, H., H. Funke, T. Bruin, H. Bucher, A. von Eckardstein, J. J. Kastelein, and G. Assmann. 1996. Compound heterozygosity for a known (D250N) and a novel (E410K) missense mutation in the C-terminal domain of lipoprotein lipase causes familial chylomicronemia. *Hum. Mutat.* **8:** 381–383.
36. Buscà, R., M. Martínez, E. Vilella, P. Pognonec, S. Deeb, J. Auwerx, M. Reina, and S. Vilaró. 1996. The mutation $Gly^{142}\rightarrow$Glu in human lipoprotein produces a missorted protein that is diverted to lysosomes. *J. Biol. Chem.* **271:** 2139–2147.
37. Auwerx, J. H., S. Deeb, J. D. Brunzell, G. Wolfbauer, and A. Chait. 1989. Lipoprotein lipase gene expression in THP-1 cells. *Biochemistry.* **28:** 4563–4567.
38. Kundel, T. A., J. D. Roberts, and R. A. Zakour. 1987. Rapid and efficient site-specific mutagenesis without phenotypic selection. *Methods Enzymol.* **154:** 367–382.
39. Miyazaki, J. I., K. Takaki, F. Tashiro, A. Tominega, K. Takatsu, and K. Yamamura. 1989. Expression vector system based on the chicken-actin promoter directs efficient production of interleukin-5. *Gene.* **79:** 269–277.
40. Niwa, H., K. Yamamura, and J. Miyazaki. 1991. Efficient selection for high-expression transfects with a novel eukaryotic vector. *Gene.* **108:** 193–200.
41. Kriegler, M. 1990. Gene Transfer and Expression: A Laboratory Manual. M. Stockton Press, New York. 99–100.
42. Buscà, R., J. Peinado, E. Vilella, J. Auwerx, S. S. Deeb, S. Vilaró, and M. Reina. 1995. The Mutant $Asn^{291}\rightarrow$Ser human lipoprotein lipase is associated with reduced catalytic activity and does not influence binding to heparin. *FEBS Lett.* **367:** 257–262.
43. Liu, M. S., Y. Ma, M. R. Hayden, and J. D. Brunzell. 1992. Mapping of the epitope on lipoprotein lipase recognized by a monoclonal antibody (5D2) which inhibits lipase activity. *Biochim. Biophys. Acta.* **1128:** 113–115.
44. Vilella, E., J. Joven, M. Fernández, S. Vilaró, J. D. Brunzell, T. Olivecrona, and G. Bengtsson-Olivecrona. 1993. Lipoprotein lipase in human plasma is mainly inactive and associated with cholesterol-rich lipoproteins. *J. Lipid. Res.* **34:** 1555–1564.

45. Ramírez, I., A. J. Kryski, O. Ben-Zeev, M. C. Schotz, and S. L. Severson. 1985. Characterization of triacylglyceride hydrolase activities in isolated myocardial cells. *Biochem. J.* **232:** 229–236.
46. Nilsson, T., J. M. Lucocq, D. Mackay, and G. Warren. 1991. The membrane spanning domain of β-1,4-galactosyltransferase specifies *trans* Golgi localization. *EMBO J.* **10:** 3567–3575.
47. Eisenberg, D., and A. D. McLachlan. 1987. Solvation energy in protein folding and binding. *Nature.* **319:** 199–203.
48. Krapp, A., H. Zhang, D. Ginzinger, M-S. Liu, A. Lindberg, G. Olivecrona, M. R. Hayden, and U. Beisiegel. 1995. Structural features in lipoprotein lipase necessary for the mediation of lipoprotein uptake into cells. *J. Lipid. Res.* **36:** 2362–2373.
49. Helenius, A., T. Marquardt, and I. Braakman. 1992. The endoplasmic reticulum as a protein-folding compartment. *Trends Cell Biol.* **2:** 227–231.
50. Kozaki, K., T. Gotoda, M. Kawamura, H. Shimano, Y. Yazaki, Y. Ouchi, H. Orimo, and N. Yamada. 1993. Mutational analysis of human lipoprotein lipase by carboxyl-terminal truncation. *J. Lipid. Res.* **34:** 1765–1772.
51. Richardson, J. S., and D. C. Richardson. 1989. Principles and patterns of protein conformation. *In* Prediction of Protein Structure and the Principles of Protein Conformation. G. Fasman, editor. Plenum Press, New York. 1–98.
52. Lo, J. Y., L. C. Smith, and L. Chan. 1995. Lipoprotein lipase: role of intramolecular disulfide bonds in enzyme catalysis. *Biochem. Biophys. Res. Commun.* **206:** 266–271.
53. Flynn, G. C., J. Pohl, M. T. Flocco, and J. E. Rothman. 1991. Peptide-binding specificity of the molecular chaperone BiP. *Nature.* **353:** 726–730.
54. Gaut, J. R., and L. M. Hendershot. 1993. The modification and assembly of proteins in the endoplasmic reticulum. *Curr. Opin. Cell Biol.* **5:** 589–595.
55. Brewer, J. W., and R. B. Corley. 1996. Quality control in protein biogenesis: thiol-mediated retention monitors the redox state of proteins in the endoplasmic reticulum. *J. Cell Sci.* **109:** 2383–2392.
56. Fra, A. M., C. Fagioli, D. Finazzi, R. Sitia, and C. M. Alberini. 1993. Quality control of ER synthesized proteins: an exposed thiol group as a three-way switch mediating assembly, retention and degradation. *EMBO J.* **12:** 4755–4761.
57. Isidoro, C., C. Maggioni, M. Demoz, A. Pizzagalli, A. M. Fra, and R. Sitia. 1996. Exposed thiols confer localization in the endoplasmic reticulum by retention rather than retrieval. *J. Biol. Chem.* **271:** 26138–26142.
58. Marquardat, T., and A. Helenius. 1992. Misfolding and aggregation of newly synthesized proteins in the endoplasmic reticulum. *J. Biol. Chem.* **117:** 505–513.
59. Ma, Y., T. C. Ooi, M-S. Liu, H. Zhang, R. McPherson, A. L. Edwards, I. J. Forsythe, J. Frohlich, J. D. Brunzell, and M. R. Hayden. 1994b. High frequency of mutations in the human lipoprotein lipase gene in pregnancy-induced chylomicronemia: possible association with apolipoprotein E2 isoform. *J. Lipid. Res.* **35:** 1066–1075.
60. Coleman, T., R. L. Seip, J. M. Gimble, D. Lee, N. Maeda, and C. F. Semenkovich. 1995. COOH-terminal disruption of lipoprotein lipase in mice is lethal in homozygotes, but heterozygotes have elevated triglycerides and impaired enzyme activity. *J. Biol. Chem.* **270:** 12518–12525.